NAVAL RESEARCH

REVIEWS

JULY 1975

PROFILES IN SCIENCE

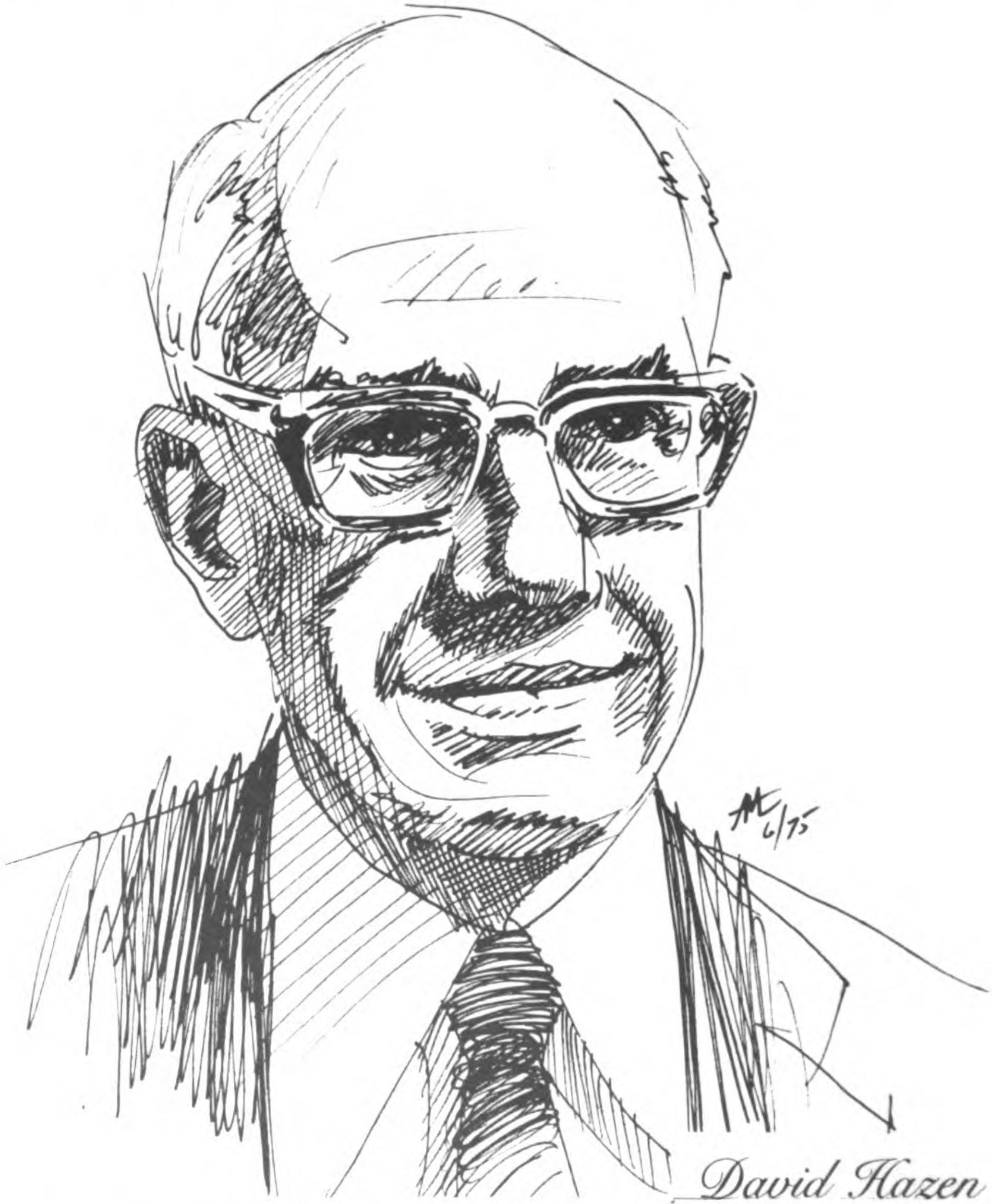

David Hazen is Professor of Aeronautical Engineering at Princeton University; his field of interest is low speed aerodynamics with emphasis on vertical-takeoff and short-takeoff and landing (V/STOL) aircraft. In 1951 Professor Hazen conducted a study for the Office of Naval Research on the flow mechanisms associated with circulation control of wings. Several years later he developed a plan to use a blimp as a "flying wind tunnel" to conduct tests on models of V/STOL aircraft. These tests were very successful in verifying wind tunnel data.

Professor Hazen has had an influential role in organizing foreign educational institutions. He established the Aeronautical Engineering Department at the Indian Institute of Technology, and the College of Petroleum and Minerals in Arabia, and is trustee of Robert College in Istanbul.

Today Professor Hazen continues to work for the Navy as Chairman of the Naval Research Advisory Committee, of which he has been a member since 1968.

Microwave Signal Processing with Resonant Echo Phenomena

D. E. Kaplan*
Lockheed Palo Alto Research Laboratory

The discovery of magnetic resonance in the mid-1940's provided a powerful new method for studying the interactions of nuclei and electrons in liquids and solids and spawned spectroscopic techniques that are now widely used for chemical and biological analysis in science and industry. Resonance principles soon found important application to such areas as magnetometers for precise magnetic field measurement and masers for low-noise microwave amplification.

Experiments which detected the resonance absorption of energy from a continuous wave source at frequencies appropriate to the interaction of the nuclear or electron magnetic moment and an applied magnetic field (continuous wave magnetic resonance experiments) were followed in the early 1950's by a variety of pulsed or transient resonance experiments. In such experiments, a specimen containing a large number of nuclear or electron spins (commonly denoted spin system or spin ensemble) is excited by one or more pulses of resonance radiation. Measurements are made of energy absorbed during pulse application or of radiation emitted after the pulses have been applied. In the course of one such transient resonance experiment, E. L. Hahn (who is now Professor of Physics at The University of California, Berkeley) made the remarkable discovery (1) that application of a sequence of two or three resonant pulses to a nuclear spin system resulted in the delayed occurrence of phase coherent states among the spin ensemble. The large macroscopic magnetic moment associated with this condition of phase coherence radiates strongly, and the attendant pulse is termed as spin echo. Figure 1 illustrates the characteristic sequence for this echo experiment. The envelope of the echo amplitude formed as the pulse interval is varied was shown by Hahn to reveal directly phase and energy relaxation rates of the spin ensemble. Echo resonance techniques rapidly became a widely utilized tool for the time domain study of relaxation and diffusion processes in spin systems. In related echo experiments, the nuclear and electronic environment of a resonant species could be studied through its

*Dr. D. E. Kaplan is a Senior Member of the Lockheed Palo Alto Research Laboratory. Dr. Kaplan's research interests have been largely concerned with coherent pulse stimulated radiation phenomena, particularly echo effects and their application as a means for the correlation, delay, and amplification of microwave signals.

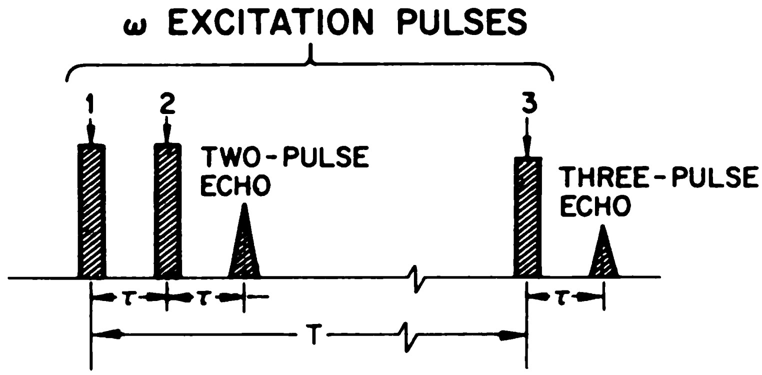

Figure 1 — Two-pulse and three-pulse echo sequence

effect upon the echo envelope, and weakly abundant neighboring spin systems could be identified in sensitive double resonance experiments by means of echo observations on a dominant indicator species.

The generation of an echo following the application of two or more pulses is an inherently nonlinear process. That is, the spin system which produces the echo must respond to the pulse stimulation in a manner which is *not* directly proportional to the magnitude of the excitation. In the case of a linear response characteristic, the output would simply represent the summation of responses to the separate pulse excitations. A delayed emitted pulse, or echo, cannot be constructed from a linear response. In the case of a two-level spin system (two allowed energy states between which magnetic transitions occur) the dominant nonlinearity is associated with the amplitude response of the spin system to the stimulating pulses. Hahn's apt racetrack analogy for echo formation, of runners symbolizing spins with distributed characteristic frequencies reversing direction at the time of the second pulse and later regrouping at the original starting line, will be familiar to many readers. Similar two-level quantum systems, whether they be magnetic dipole, or electric dipole as in the case of the photon echo, (2) may be described in a like manner and will produce echoes with parallel properties.

Following the discovery of the spin echo, it was recognized that this phenomenon also constituted a unique form of digital memory, permitting the controlled storage and recall of radio frequency pulses. Investigations of the potential for radio frequency signal processing and digital memories (3,4) based upon nuclear echo phenomena were undertaken early in the evolution of echo technology. In contrast with its wide application as a diagnostic tool for fundamental studies, the nuclear spin echo did not become competitive with alternative technology for device application, but interest has persisted in the possible utilization of related phenomena in other physical media with resonant frequencies lying in the microwave or optical spectral regions.

With the maturation of electron resonance techniques and the advent of a variety of laboratory instrumentation suitable for pulsed microwave experiments, investigation of the microwave analogue of the nuclear spin echo in electron spin systems was undertaken at the Lockheed Palo Alto Research Laboratory under the sponsorship of the Office of Naval Research. At the time the study was initiated, the intent was to investigate the feasibility of a microwave computer memory based upon the echo technique. Various proposals for computer logic elements employing microwave carriers rather than baseband signals for information processing were then under active study. Interest in this type of computer technology has since waned but certain results of this program, which now continues in a different format, are important because they illustrate how a research project can lead into productive new areas yielding results of an entirely unanticipated nature, in this case with a potential for application to microwave signal processing devices.

A pulsed microwave resonance spectrometer, in many respects similar to a high resolution radar system, was developed to display transient electron resonance phenomena. Because of the strength of electron interactions, electron spin echoes were expected to have coherent lifetimes on the order of microseconds, rather than the millisecond lifetime characteristic of nuclear spin phase memory. During this program, which initiated with an examination of narrow linewidth paramagnetic systems at low temperature, other resonant physical systems with an intrinsically high-Q response, but of a different physical character than two-level quantum systems, were subject to multiple pulse excitation. Surprisingly, in several cases echo phenomena were observed bearing the same temporal relationship to the stimulating pulses as that of spin echo but with unusual envelope and intensity properties. The most notable examples from this study are the cyclotron echo (5) from free electrons in various magnetoplasma regimes and echoes from spin modes representing collective magnetic behavior in ferrimagnetic (6,7) material.

The cyclotron resonance of charged particles at low excitation energies and low density is understood to be a linear phenomenon and should not produce echoes. In fact, the cyclotron echo appeared as a particularly strong effect with a radiated power level that could reach 1 to 2% of that of the excitation pulses, and uncharacteristically the echo amplitude initially grew rapidly as the pulse separation was increased from minimum intervals. This led to a search for other types of physical processes that could produce echoes. The cyclotron echo proved to be the first experimental example of several new types of echo-producing mechanisms which include nonlinear relaxation, amplitude-dependent oscillator frequency shifts, and localized oscillator coupling. Space precludes a discussion in this article of the physics underlying these novel echo formation mechanisms, but the interested reader is referred to the abundant literature on the subject (8-13). It is instructive to note here that the mechanisms cited all become operative during the oscillator phase drift period after pulse application, with the result that the echo amplitude grows with increasing pulse separation as the cumulative effect of the echo-producing process enhances the strength of the coherent moment. Eventually relaxation effects irreversibly dissipate energy, and the echo decays. This behavior is in striking contrast to that of the spin echo, whose origin is due to a nonlinear response of the spins during the pulse application. The spin echo amplitude decays monotonically as the pulse interval is increased.

We now turn our attention to the ferrimagnetic echo (14), which, because of a peculiar combination of experimental parameters, appears to be the most promising candidate for device application within this family of echo phenomena that have been investigated to date. Certain of these device-oriented studies are conducted under the sponsorship of the Naval Research Laboratory. The ferrimagnetic echo, first observed in narrow linewidth yttrium iron garnet (YIG), shares with the cyclotron echo the unusual envelope characteristic and exhibits an altogether singular amplification phenomenon (7, 12-15). For a limited range of pulse interval, the echo intensity can be two to three orders of magnitude greater than that of the input signal. This amplification has been observed over a wide frequency range extending into microwave X-band at ambient temperature, and over appreciable instantaneous bandwidths of several hundred MHz or more. The amplification process results from active mode coupling (12,13) within a restricted portion of the spin wave spectrum. A coupled mode ensemble can be shown to exist (16) in a bounded sample geometry with the coupling characteristically localized in both frequency and space throughout the mode spectrum. The coupling between spin modes with low oppositely directed group velocities of similar magnitude provides positive feedback with some modes gaining energy rapidly at the expense of others. This is in effect a many bodied parametric amplification process and the experiment provides an unusual example of a time domain ferrimagnetic amplifier in which both signal and "pump" are applied in the same frequency range. The system may be likened to an array of pendula of progressively spaced characteristic frequency, each spring coupled to its adjacent neighbors in frequency and space. The energy for the amplified echo is derived from the second pulse in a two-pulse sequence or the third pulse in a three-pulse sequence. The peak power of this pump pulse may generally be of the order of 1 watt or less and signal pulse powers may lie in the range from 10^{-12} to 10^{-5} watts for linear amplification. Signal gain on the order of 20 to 30 dB is not uncommon at frequencies from 1 to 10 GHz. At frequencies where the YIG linewidth is minimized, echo amplification may be observed for echo-signal intervals of as much as several microseconds.

The localized coupling of the spin modes producing the amplified echo requires an internally inhomogeneous magnetic field. The field conditions are found to be conveniently satisfied by combining the effects of internal gradients arising from surface demagnetizing fields in crystal geometries of modest aspect ratio with small permanent magnets which themselves provide a bias field having both longitudinal and transverse field gradients. An example of such a configuration which produces strong amplified echoes is shown in Figure 2. High energy product samarium cobalt disk magnets bracket a short YIG bar and associated meanderline microwave coupling structure. While this geometry has some limitations for device application, it serves to illustrate how compact the assembly can be made. The YIG delay element can be formed from a composite matrix consisting of a polycrystalline component in which a small single crystal segment is imbedded at a location where the field gradients are conducive to amplified echo generation. Figure 3 is a typical two-pulse amplified echo sequence from a composite YIG bar in a slightly larger permanent magnet geometry yielding amplification at upper C-band frequencies.

Figure 2 – Experimental miniature ferrimagnetic echo module using rare earth magnets

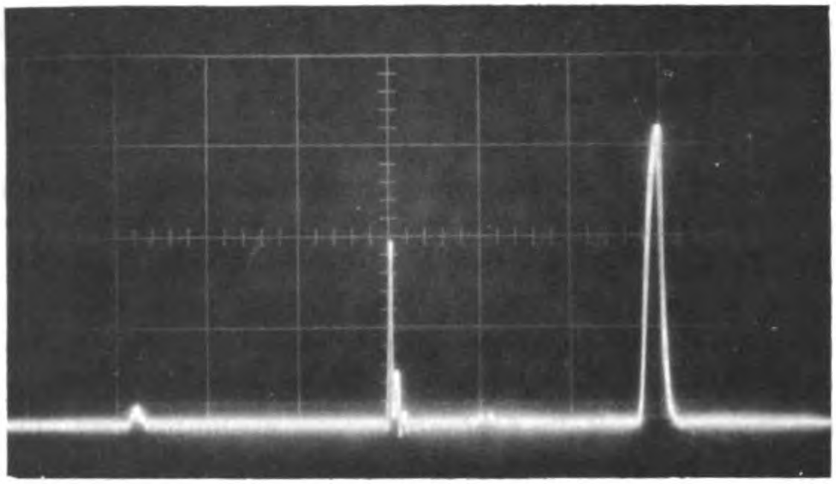

Figure 3 – Oscilloscope display of amplified echo from 1-mm single-crystal YIG wafer positioned 2.5 mm from polycrystalline YIG bar end face. Echo gain is approximately 20 dB for delay time 2τ of 1.2 μsec. P_2 is of 15-nsec duration with peak power of 1 W. Receiver gain is electronically reduced during P_2 on-time.

While the echo delay and amplification process is inherently volatile and lifetime limited by relaxation effects, it is possible to prolong signal storage with an iterative pulse sequence in which a signal is first amplified and then kept alive in the crystal for periods in excess of 10 microseconds.

The delay and amplification of a monochromatic pulse as shown in Figure 3 is a form of cross correlation process which provides signal replication when the second pulse approximates a delta function. A modified form of autocorrelation (17) with signal gain can be obtained if the pump pulse is one-half the time duration of the signal and has the same frequency characteristics. These pulse sequences are illustrated in Figures 4 and 5 for monochromatic and chirped waveforms, respectively, and typical experimental results are shown in Figures 6 and 7. Time bandwidth products for pulse compression in excess of several hundred have been obtained with the chirped signals. An echo representing a dispersive display or spectral signature of a short signal pulse can be obtained by following the signal with a chirped processing pulse as shown by reading Figure 5 from right to left. Pulse compression and pulse expansion sequences may be successively combined to provide pulse time multiplexing and demultiplexing of a digital signal pulse code, spaced both in frequency and time.

The evolution of an attractive signal processing device based upon the ferrimagnetic echo is complicated by the fact that the most interesting device configurations have, due to their compactness, many

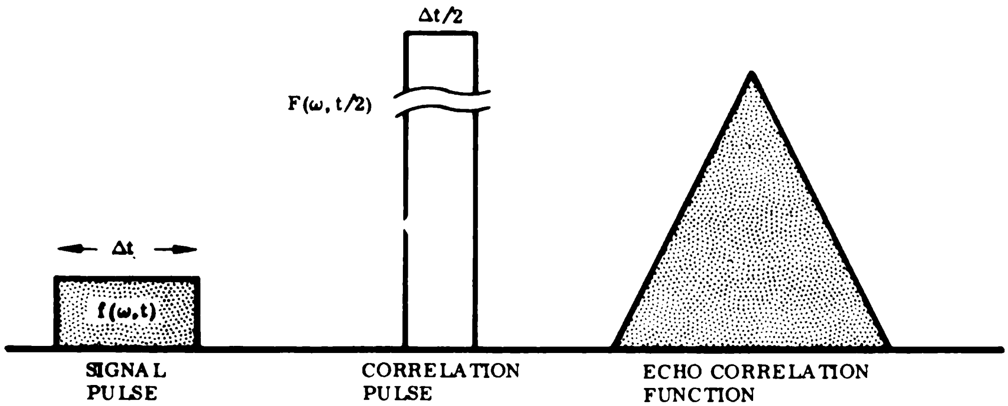

Figure 4 — Autocorrelation sequence for monochromatic signal pulse

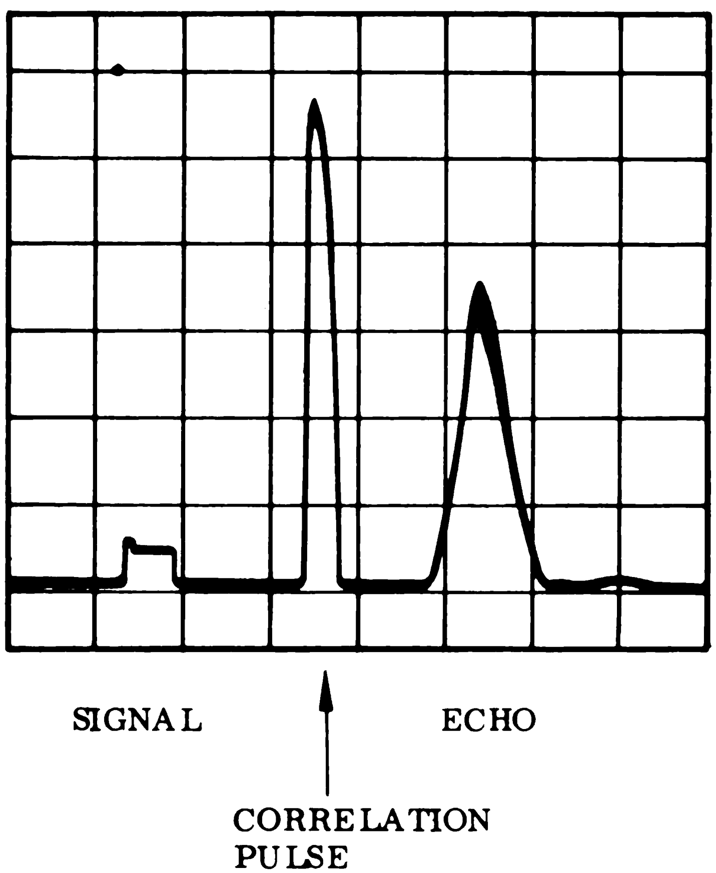

Figure 5 — Autocorrelation sequence for chirped signal pulse

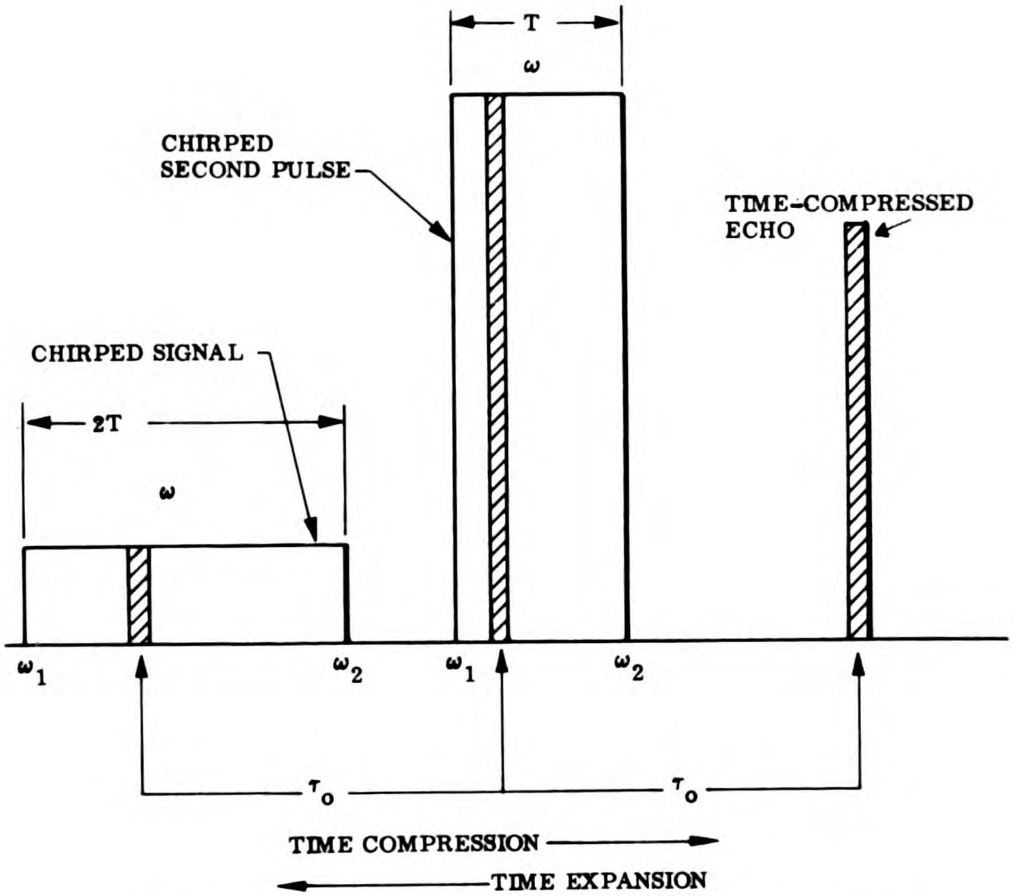

Figure 6 – Experimental display of autocorrelation of monochromatic pulse at 7 GHz. Time scale is 200 nsec/cm.

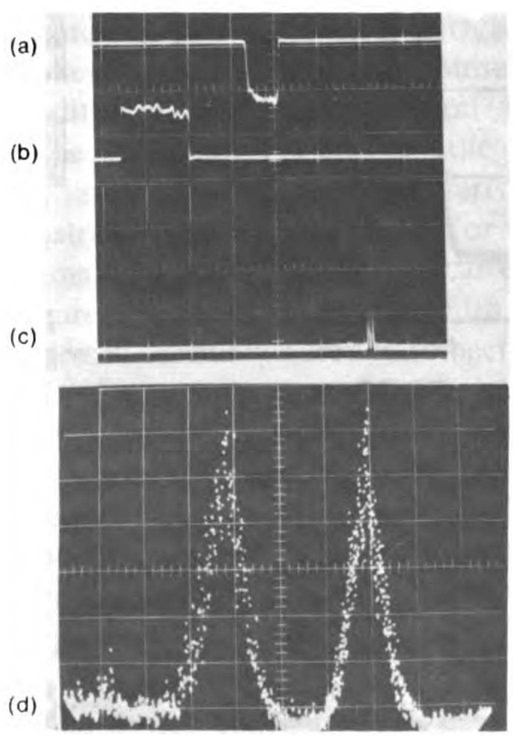

Figure 7 – Experimental display of echo pulse compression at 9 GHz. Frames a, b, c show processing pulse, signal, and echo, respectively. The signal is a composite of two chirped pulses with a 15-nsec relative displacement and is externally amplified for presentation. Time scale is 0.5 μ/cm. Frame d at 5 nsec/cm is a time-expanded display of the doublet echo.

different field gradient components and do not readily lend themselves to an analytical treatment. As an inherently active signal correlator, its application to signal processing systems poses problems not usually encountered with a passive device. Notwithstanding these circumstances, the features of room temperature amplification, small physical size, modest pump power, and electronically variable delay are quite unique in combination and invite a serious effort toward ferrimagnetic echo device development.

References

1. Hahn, E.L., *Phys. Rev.* **80**, 580 (1950)
2. Kurnit, N.A., Abella, I.D., and Hartmann, S.R., *Phys. Rev. Let.* **13**, 567 (1964)
3. Anderson, A.G., Garwin, R.L., Hahn, E.L., Horton, J.W., Tucker, G.L., and Walker, R.M., *J. Appl. Phys.* **26**, 1324 (1955)
4. Fernbach, S., and Proctor, W., *J. Appl. Phys.* **26**, 170 (1955)
5. Hill, R.M., and Kaplan, D.E., *Phys. Rev. Let.* **14**, 1062 (1965)
6. Kaplan, D.E., *Phys. Rev. Let.* **14**, 254 (1965)
7. Kaplan, D.E., Hill, R.M., and Herrmann, G.F., *Phys. Rev. Let.* **26**, 1156 (1968)
8. Herrmann, G.F., and Whitmer, R.F., *Phys. Rev.* **143**, 122 (1966)
9. Herrmann, G.F., Hill, R.M., and Kaplan, D.E., *Phys. Rev.* **156**, 118 (1967)
10. Gould, R.W., *Am. J. Phys.* **37**, 585 (1969)
11. Harp, R.S., Bruce, R.L., and Crawford, F.W., *J. Appl. Phys.* **38**, 3385 (1967)
12. Herrmann, G.F., Kaplan, D.E., and Hill, R.M., *Phys. Rev.* **181**, 829 (1969)
13. Herrmann, G.F., Hill, R.M., and Kaplan, D.E., *Phys. Rev.* **B2**, 2587 (1970)
14. Kaplan, D.E., Hill, R.M., and Herrmann, G.F., *J. Appl. Phys.* **40**, 1164 (1969)
15. Deryugin, I.A., Nechiporuk, Y.A., and Tychinskii, A.V., Sov. *Phys. Solid State* **14**, 264 (1972)
16. Vasile, C.F., and LaRosa, R., *J. Appl. Phys.* **39**, 1863 (1968)
17. Mims, W.B., *Proc. IEEE* **51**, 1127 (1963)

Nylon-11 May Be Ideal High Pressure Lube

Dr. L. C. Towle of the Naval Research Laboratory reports that Nylon-11 may be an ideal lubricant for high pressure applications, and it won't break down as easily as other solid films presently in use, such as fluoroethylenes.

The solid film lubricant promises to have many applications for the Navy and industry. The use of solid film lubricants has become increasingly common in the last decade, particularly in special applications where conventional greases and oils lose their effectiveness due to high stress conditions. The finite shear strength of a solid film retards its expulsion from regions of high stress and helps maintain the integrity of the lubricant film.

(Continued on Page 29)

588-356-O - 75 - 2

Ignition of Hydrocarbons and the Thermalization of Electrical Discharges*

E. Barreto, S. I. Reynolds, and H. Jurenka†
State University of New York at Albany

This research on electrical discharges began in an effort to find the maximum electrical charge that could be placed on a water drop. The Office of Naval Research supported the project because it would benefit the Navy in dealing with the problems of fog forecasting and thunderstorm phenoemna. Today the research continues with the broader objectives of understanding the mechanism of electrical breakdown in a charged mist or aerosol so as to be able to distinguish between the conditions that lead to corona or brush discharge and single streamer or spark discharge. There are several aspects to the naval relevance of this research including the provision of better data for design against the hazard of direct lightning strike or simply the breakdown of plastic or dielectric surfaces, such as a windshield in strong electric field conditions. Communications interference and tanker explosions are other applicable areas for the research.

The principal approach to this research is through laboratory simulation experiments in which spark currents and luminosities are very closely timed and the sparks photographed. Both metallic and dielectric electrodes are used and also electrodes of fresh and saline water.

Electrical discharges between metal electrodes are very efficient and convenient ignition sources, and their ability to ignite has been carefully evaluated (1). Recently, need has increased to determine the properties of the electrical discharges that produce unwanted ignitions when nonmetal surfaces are involved. The oil industry, for instance, has suffered losses because of unexplained explosions that have been traced down to possible electrical discharges (2,3). This has added interest to well-known problems associated with ignitions in coal mines, flour mills, and operating rooms where such discharges

---

*Mr. Barreto is a Science Research Associate at the State University of New York. His fields of interest are electrical discharges and aerosols. Mr. Reynolds, who formerly was at the Research and Development Center of General Electric, is now a Research Associate at the University. Mr. Jurenka is a graduate student assisting with the project.

†This article has been extracted from the Journal of Applied Physics, Vol. 45, No. 8, August 1974, page 3317.

are recognized sources of trouble. Also, the prolific use of all kinds of plastics and epoxy coatings provides an increasing probability for the occurrence of unwanted stored charges and possible discharges. These have caused problems, most of the time unexpected and sometimes affecting large-scale projects. For instance, charge accumulation on the bigger windshield of new large aircraft can produce punctures that could cause a loss of pressure in the pilot's cockpit (4,5). Also, electrical discharges were found to be the cause of potential problems in the Apollo and Skylab spacecrafts (6).

In this report we study the physical mechanism by which electrical discharges ignite hydrocarbons, and propose an ignition criterion that is based on the properties of the discharge channel.

Experimental Setup

The experiments are done using electrodes of different shapes to control the geometrical distribution of the electric field in the discharge gap. A uniform field is approximated by a sphere-plane configuration instead of two planes. The diameter of the sphere used is about 25 times the gap separation (2mm) and the breakdown voltage is the same using either this sphere or two plane electrodes. The use of the sphere is preferred because it localizes the region of breakdown. For tests using a liquid surface, a thin rubber gasket is placed on top of a plane metal electrode and the circular region inside the gasket is filled with water. For tests using a solid dielectric, a 0.01-cm-thick polyester film (Mylar) is placed on top of the lower plane electrode.

The electrical circuit is shown in Figure 1. The power supply is connected to the gap through a very large resistor. Therefore, the energy for the rapid discharges is supplied only by a capacitor C that represents the sum of several capacities all in parallel: the electrode gap (2-3 pF), the wires and associated supports (10 pF) and capacity purposely added to the circuit. The values are measured using a bridge that was specially constructed for this purpose (7) and is accurate to ± 0.5 pF.

The discharge is monitored using a still camera, a photomultiplier, and a fast oscillosoope that reads the voltage across a small series resistor (50Ω). It can be shown that the motion of charge in the interelectrode gap is accurately reproduced by the current flow in this resistor, and that the trace on the oscilloscope measures the development of the discharge current from onset even before the charges produced in the gap can reach the electrodes.

For tests producing ignitions, the electrode gap is enclosed in a Lucite tube that has a flexible cover. Only propane-air mixtures are

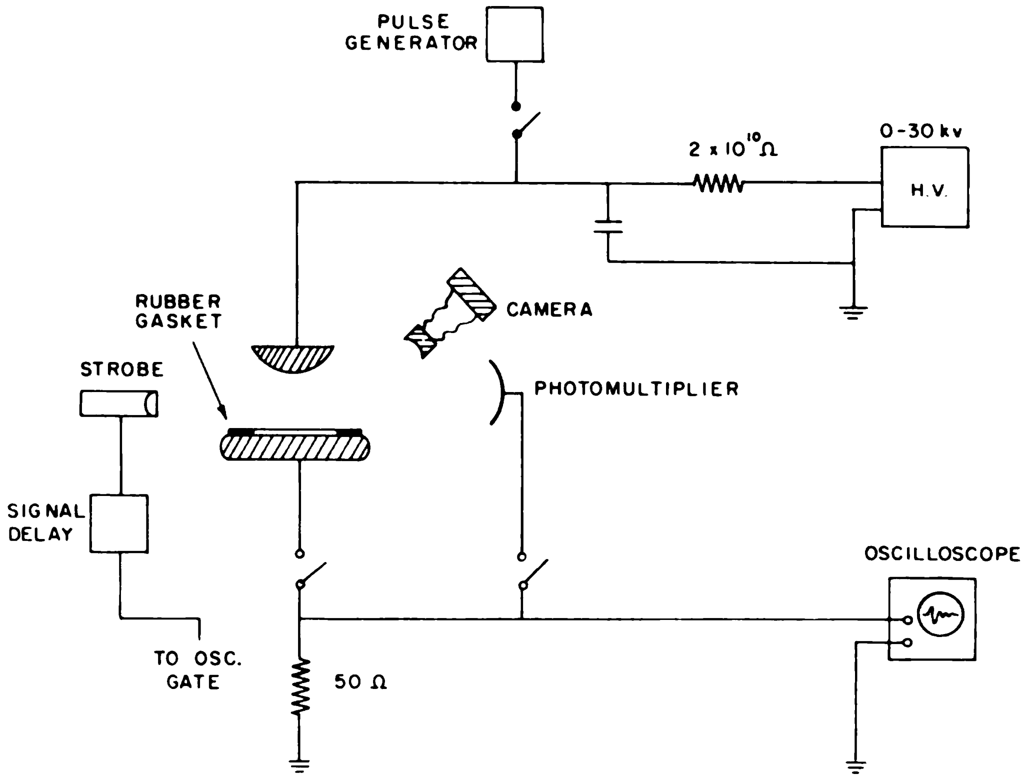

Figure 1 — Experimental setup

used at a constant mixing ratio of 5.5% propane by volume. The minimum energy values experimentally obtained are in the range of tenths of millijoules and close to those published in the literature (1). This shows compatibility of our tests with those using more elaborate control of the gas mixture.

Hydrocarbon Explosions

The ignition of a hydrocarbon-air mixture happens because free radicals (e.g., H, OH, CH's, COH's) are able to break up the C-H chains. The initial breakup is accompanied by the release of chemical energy that heats the system while the chemical reactions are producing new free radicals. Since the reaction rates for the chemical transformations are rapidly increasing functions of temperature, heat is produced at an increasing rate and, if the mixture is appropriate, the overall pressure of the system changes very rapidly. That is, an explosion takes place. This description is simplistic but serves to illustrate basic ignition properties that are important when considering electrical discharges. First of all, there must exist a critically sized nucleating volume for which heat conduction through its surface matches heat production in the inside. For this and smaller volumes, no significant local heating can take place and the pressure does not increase fast enough to be an explosion. The concept of a critically sized reacting volume leads, of course, to quenching distances in spark gaps (1). This is a distance below which electrical discharges do not ignite using parallel planes (2.00 mm in our 5.5% propane-air mixture). Note that the quenching distance is a basic property of the combustion process itself, not of the electrical discharge. It is clear then that ignitions are basically heat-transfer processes and as such their onset takes a long time compared to the time for an electrical discharge. Figure 2 shows the luminosity traces seen by the photomultiplier when two ignitions are produced using two different capacitances. At the sweep speed used (1 msec/div) the spark discharge is barely visible and complete at zero time. Note, however, that the luminosity from the ignition exhibits a slow rise time of the order of milliseconds compatible with heat-transfer processes in the air. In fact, the luminosity traces in Figure 2 have, as expected, the same shape as that of the temperature profile across an adiabatic plane combustion wave. Therefore, the discharge always becomes hot before the hydrocarbons can release sufficient heat to ignite the mixture by chemical reactions. In other words, the role of the spark is to raise the temperature in a critically sized volume around the discharge channel. This volume must be filled with the proper mixture in order to sustain the chemical reaction, but the heat transfer to it actually takes place long after the electrical event has concluded, as seen in the luminosity traces of Figure 2. Conversely, when an electrical discharge produces an ignition, this demonstrates that the character of the discharge is such that electrical energy has been transformed into heat along a discharge filament.

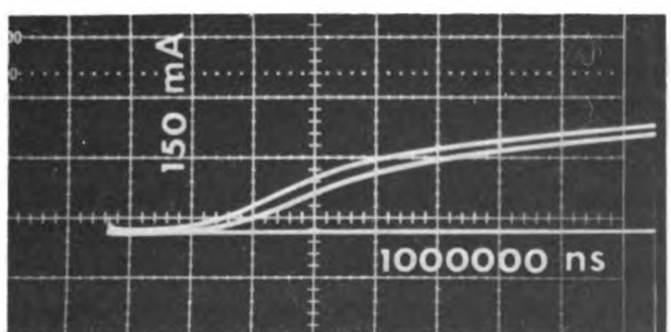

9.15 kv 33 and 133 pf

Figure 2 – Photomultiplier signal from the light accompanying two ignitions with different capacities. A metal-water gap is used. Note the spark is over at practically zero time and long before light from the ignition appears.

Thermalization of the Discharge Channel

The thermalization process that converts part of the electrical energy stored in the capacitor into thermal energy of the gas is not completely understood. The oscilloscope trace of Figure 3 shows the current measured as a function of time using metal electrodes and a uniform electric field. The gap separation is the quenching distance (0.2 cm), and an ignition takes place a few milliseconds after the recorded trace. Figure 3 shows that the whole heating process from onset takes less than 40 nsec. The area under this current-vs-time trace represents the charge stored in the capacitor. Since ignition tests have shown that the heat loss to the electrodes is small (1), and since the Joule energy going into the test resistor is also small compared to the energy stored in the capacitor, we can be sure that most of the energy has gone into the gas. The field is significantly higher than the conventionally quoted breakdown strength for air (40 vs kV/cm) not because of the gas mixture but because of the small gap used.

The electrical discharge is completed very early in the ignition sequence, and the times of interest, as far as the production of a small heated volume is concerned, range not in milliseconds but in tens of nanoseconds. This assumes that there is no process whereby electrical energy is transferred to the gas and stored in it for nearly a millisecond before the gas temperature increases. The only process that we can envision as capable to produce such an effect is the production of metastable molecules. In fact, it is known that metastables can affect the onset conditions in a sequence of several discharges, but this only proves that the total metastable stored energy per single discharge is small compared to the thermal energy of the gas. The possibility of

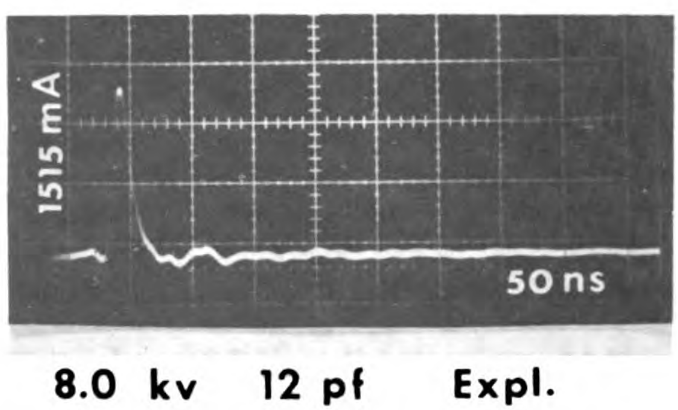

Figure 3 — Current trace from a spark that produces an ignition with minimum energy input (0.38 mJ) using metal electrodes and a uniform electric field.

direct hydrocarbon radical formation by electronic impact can be excluded by noting that in air at atmospheric pressure, the hydrocarbons are outnumbered by oxygen and nitrogen molecules. Accordingly, in a discharge, collisions by field accelerated electrons produce almost exclusively N_2 spectra (2nd positive band) even though the O_2 excitation potential is lower than that of N_2 molecules. In other words, we can be sure that N_2-electron collisions will dominate all field induced collisions because of the small ratio of hydrocarbon to N_2 molecules required to have a combustible mixture in air (about 1:17).

Ignitions produced by heating the gas by passing current through small wires of diameters comparable to those of the electric discharge (tens of microns) have shown that the wire actually melts before ignitions occur. Times for ignition are of the order of 10 ms. (Ref. 1, p. 360). This shows that within the much smaller times characteristic of sparks (50 ns) there is no significant heat transfer by molecular collisions in the gas; also, that the heating is done essentially at constant volume. This is, of course, consistent with the subsequent generation of a shock wave (an adiabatic process) and with a computed very small distance (2.5×10^{-3} cm) that molecular ions can move within the allowed time and under the influence of the applied field. The heating of the discharge channel is done exclusively by electrons because only they have time to move and store kinetic energy within the observed experimental times. Heating is then determined by dielectric properties of the gas, and these are only slightly affected by the hydrocarbon molecules due to their small relative concentration. For instance, within our experimental accuracy, we see no difference in the breakdown voltage for air or air-propane combustible mixtures. The transit time of electrons across the whole discharge gap is of the order of 10 ns. Therefore, the possibility of gradual heating by electron-neutral interaction can be rejected because it would require many transit times. It follows that heating can only be accomplished when the whole electron population holds energy comparable to the thermal energy in the gas molecules. In air at atmospheric pressure the kinetic energy per electron is limited by ionizing collisions (inelastic) to a value that is roughly 10^2 times the kinetic energy of the gas molecules. There are in air at normal temperature and pressure (NTP) about 10^{19} neutral molecules per cc. Therefore, electrons require a population of about 10^{17} cm^{-3} before they can store energy comparable to the thermal energy of the neutrals. The problem of ignitions by electrical discharges becomes, then, the problem of procuring high electron densities around 10^{17} cm^{-3} in the discharge channel plus that of the transfer of their energy to the gas molecules in times of the order of 10 ns.

When an electric field reaches its critical ionization value, that depends on the shape of the electrodes, free electrons are able to procure enough energy between collisions to ionize the gas molecules. The electron avalanches produced involve energies and currents that are negligible compared to the stored electrical energy and to the successive currents in the discharge (0.1 nJ and 0.1 μA vs 0.1 mJ and 1.0 A). Electrons in an avalanche move towards the anode leaving behind a space charge of positive ions located practically at the ionization site. Most of these positive ions are inside a spherical region 30 μm in radius. When the avalanche has produced about 10^8 ions its net positive space charge produces a strongly divergent field with a magnitude ($\sim 10^6$ V/cm) that far exceeds the field imposed by the outside voltage. This field extends into the neutral region ahead of the positive space charge for a distance that is long enough to produce new ions by localized avalanches. The few free electrons required to trigger ionization are always available by photoionization of O_2 molecules with photons from decaying N_2 excited molecules generated earlier in the discharge. At this stage the avalanche has reached a critical size, and the discharge mechanism changes to a streamer mode; that is, to a discharge that is controlled by the space charge and moves very rapidly across the gap. (In uniform fields simultaneous cathode and anode directed streamers are possible when the initial avalanche starts in mid gap.) Streamer formation times are close to 10 ns, and once formed streamers can cross the quenching distance gap in 2 ns. (10^8 cm/sec velocity.) The ion electron pairs left by the streamer in the gap have a density around 10^{15} cm^{-3}. As noted, the electronic temperature may be 100 times the gas temperature, but electrons are unable to heat the gas due to their low relative concentration (10^{15} vs 10^{19} neutrals per cm^{-3}).

There is no precise explanation for the events that follow and increase the electron density to the required number, around 10^{17} cm^{-3}. We believe it is possible for the electron gas to behave as an ideal gas that is able to sustain compression waves (analogous to shock waves) that increase the electron density in the gap. Experimentally it is known that very fast luminous pulses propagating up to a fraction of the speed of light do occur. As the electron density reaches its critical value, long range Coulomb interactions become suddenly very effective, causing the electrons to have a lower kinetic energy that is equal for all particles. Under this condition the work done on the electrons is transformed into energy of the neutrals, and the temperature of the gas increases. This thermalization process has been measured to take place within 10 additional ns. The total time budget from start of the avalanche to thermalization of the channel is of the order of 22 ns and therefore consistent with the observed heating requirements for spark ignition.

Solid Dielectric Electrodes

A solid dielectric, because of its characteristic low conductivity, holds, on its surface, charge produced during the streamer stage of the discharge. This modifies the breakdown and heating process observed using metal electrodes. Figure 4(a) shows a current trace produced when a Mylar film 0.01 cm thick is placed on the grounded plane of the positive sphere-to-plane electrode. This discharge occurs at precisely the voltage at which an incendiary spark would form without the film. The trace can be recognized to be identical to that of a breakdown streamer in a point-to-plane corona discharge (8). That is, even though the field is uniformly high along the whole gap the discharge behaves like those in which the streamer propagates in a rapidly changing field. This clearly shows that in uniform fields heating is preceded by a streamer phase and suggests that the dielectric prevents thermalization by the accumulation of charge on its surface. Accordingly ignitions are never observed, and dusting of the surface after discharge evidences charge accumulation [Figure 4(b)]. The characteristic dust pattern on the cathode is that of positive streamers over a circular region. That is, when the streamer produced in the gap reaches the film it branches and propagates in the air just over the dielectric. The positive charge thus deposited on the polyester surface lowers the field in the air gap and stops the discharge before the heating can start. Increasing the voltage after the first discharge produces new discharges that look like a brush with current traces and dust patterns as seen in Figure 5. Clearly, with fixed polarity, the charge stored in the polyester film requires a higher

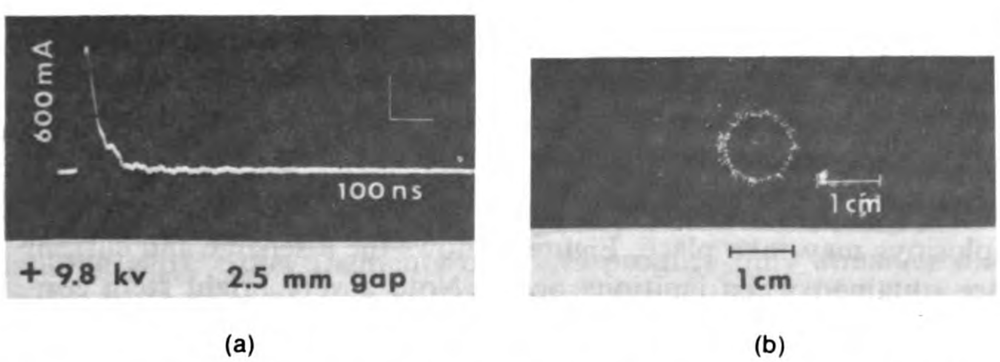

Figure 4 — Initial discharge produced in a uniform field with a polyester-covered cathode; (a) current trace, (b) positive streamer pattern produced by dusting the cathode after the discharge.

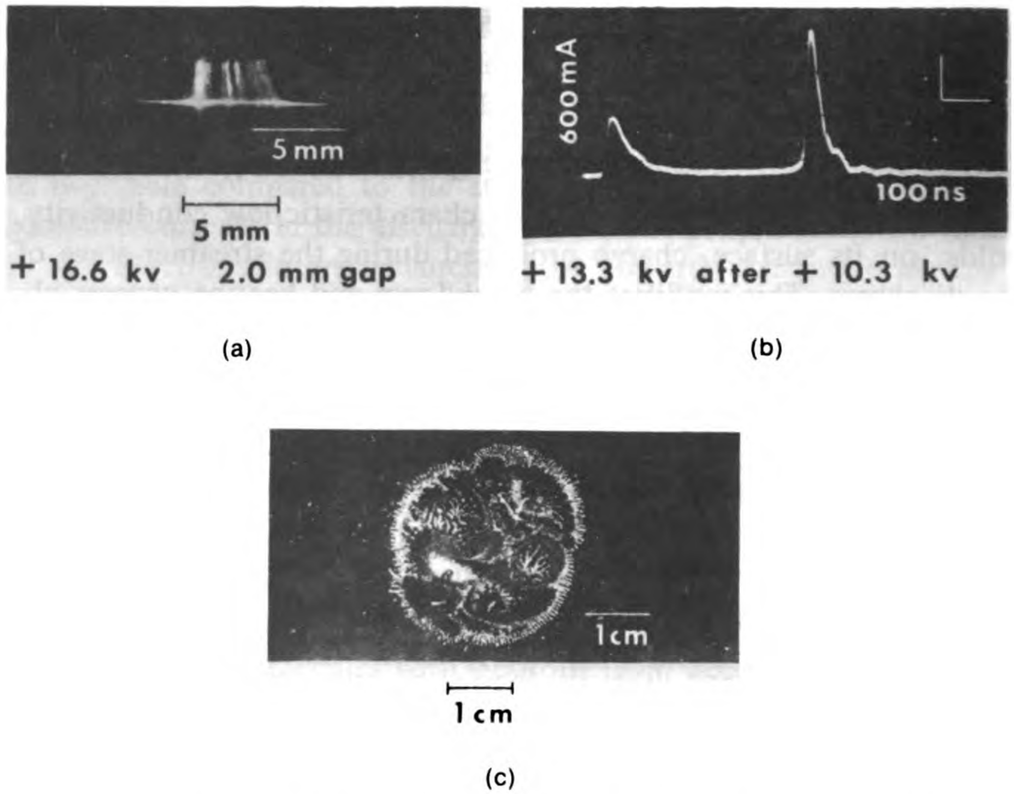

Figure 5 — Nonincendiary discharges produced after the initial one using a polyester-covered cathode. (a) Photograph using 10,000 ASA film, (b) current trace, and (c) dust figure on cathode. The pictures do not correspond to the same event.

applied voltage to procure the same ionizing field in the gap. In fact, this voltage increase can be used as a measurement of the charge on the dielectric (9-11). Since the energy supply rapidly increases with the applied voltage, a single discharge event is actually a succession of streamer discharges that provide the brushlike visual appearance. The current trace and dust pattern obtained [Figure 5 (b) and 5 (c)] show that the streamers are separated in time by several hundreds of nanoseconds, and in space each one avoids the charge deposited on the film by one previous one. As expected, these discharges do not produce ignitions because each streamer prevents its thermalization just like the first streamer in an uncharged film.

For subsequent discharges, higher voltage is always needed and explosions may take place. Figure 6 shows the discharge and current trace obtained when ignitions occur. Note a very bright stem connected to a prolifically branched surface discharge. Clearly, the charge deposited on the film eventually enhances surface streamers, allowing for the rapid feeding of charge into a single streamer channel that thermalizes and produces an ignition. With good dielectrics such

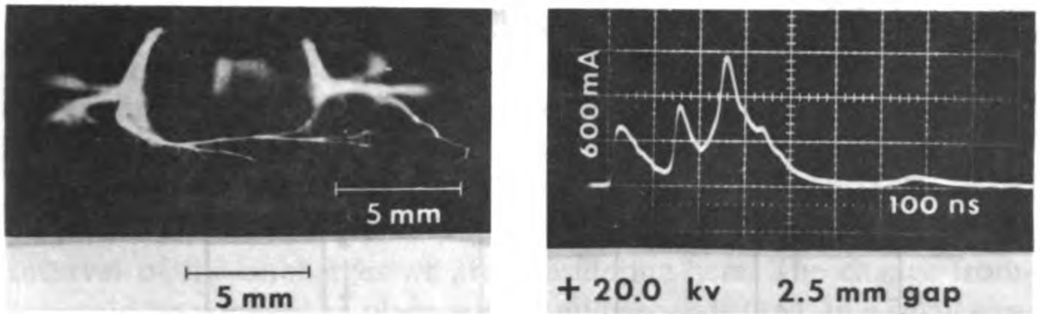

(a) (b)

Figure 6 – Incendiary discharge produced by enhanced streamer discharges over a charged polyeste -covered cathode. These discharges may be very much weaker but always exhibit prolific surface branching (a) and a finite current between streamer pulses (b).

as Mylar, Lucite, and most of the epoxy coatings used to prevent corrosion, it is possible to store the charge produced by, say, nonincendiary corona discharges over long periods of time (12). Then, polarity reversals become particularly dangerous because at very low voltages incendiary discharges may be produced. This situation as well as samples of successive trials are illustrated in the histogram in Figure 7. Note that events (E) and (F) involve 24-h time intervals. We want to note that in all cases the ignition is not produced by corona discharges, but by the collection of charge by streamers affected by charge stored on the surface of a dielectric. Similarly, ignitions can be produced by a high-voltage fast rise-time pulse applied to an isolated rod electrode. This is because the many streamer branches produced in the air feed, charge, and thermalize a single stem near the metal surface. It is interesting to note that in all these cases, regardless of the initial geometry, incendiary discharges are produced exclusively by the combined effect of many streamers propagating in asymmetric electric field configurations.

Liquid Dielectrics

Electrostatic stress causes liquids to develop either a conical shape leading to a very thin long filament about 10 μm in radius (a Taylor jet); or, an oscillating surface that periodically changes from a protruding spheroid to a sharp cone with a 49.3° semivertical angle (13). In long gaps, either filaments or cones produce only streamer discharges that do not produce ignitions. In small gaps the filaments may merely connect the electrodes through a high resistance (14). For instance, with oils we obtain no evidence of air ionization, but instead record current values that agree with Ohm's law according to the filament cross section and bulk conductivity measured. Water has

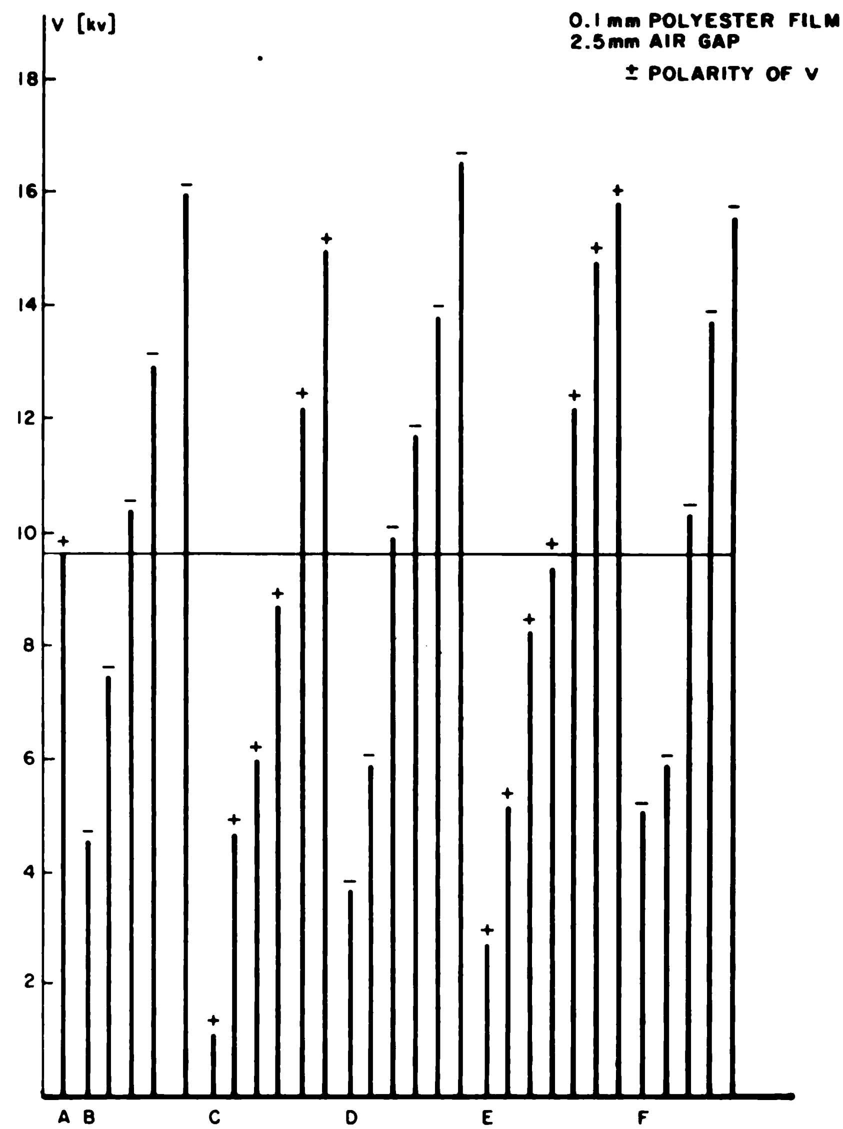

Figure 7 — Voltages required to produce successive discharges and counteract the effect of charge previously deposited by streamers on a Mylar-covered cathode. Note that changing the polarity (B, C, D, E, and F) significantly reduces the voltage required to produce a discharge. E and F were 24 h after the previous event. At the higher- and lower-voltage values the discharges are prolifically branched, hence, incendiary.

one of the highest surface tensions among all liquids. Consequently, the change from spheroid to cone takes place at such a high field that a streamer discharge is always produced at the top of the cone. In small gaps this streamer may lead immediately to an incendiary discharge. The ignitions are produced with energy higher than the minimum, but at a gap separation smaller than the quenching distance determined using flat electrodes. The same effect is observed with metal electrodes and has been ascribed to enhanced ventilation associated with more turbulent flow in a point-to-plane geometrical arrangement (1).

Figure 8 is a picture of a water surface as a spheroid in equilibrium with the applied field and also at several times following the onset of a streamer discharge from the tip of the cone. Note that the drop stays sharply conical even 2 μsec after onset, i.e., for the whole time interval of the discharges we are considering here. The change from spheroid to cone takes place within milliseconds (15). In a small gap this provides essentially a pulsed voltage that leads to breakdown with point-to-plane geometry. The voltage difference at which the discharge is produced is controlled not directly by air ionization but by the mechanical deformation that locally intensifies the field and then produces a discharge. Accordingly, Figure 9 shows that the maximum possible voltage across a given gap is much smaller than the value obtained using metal electrodes. The corresponding current traces

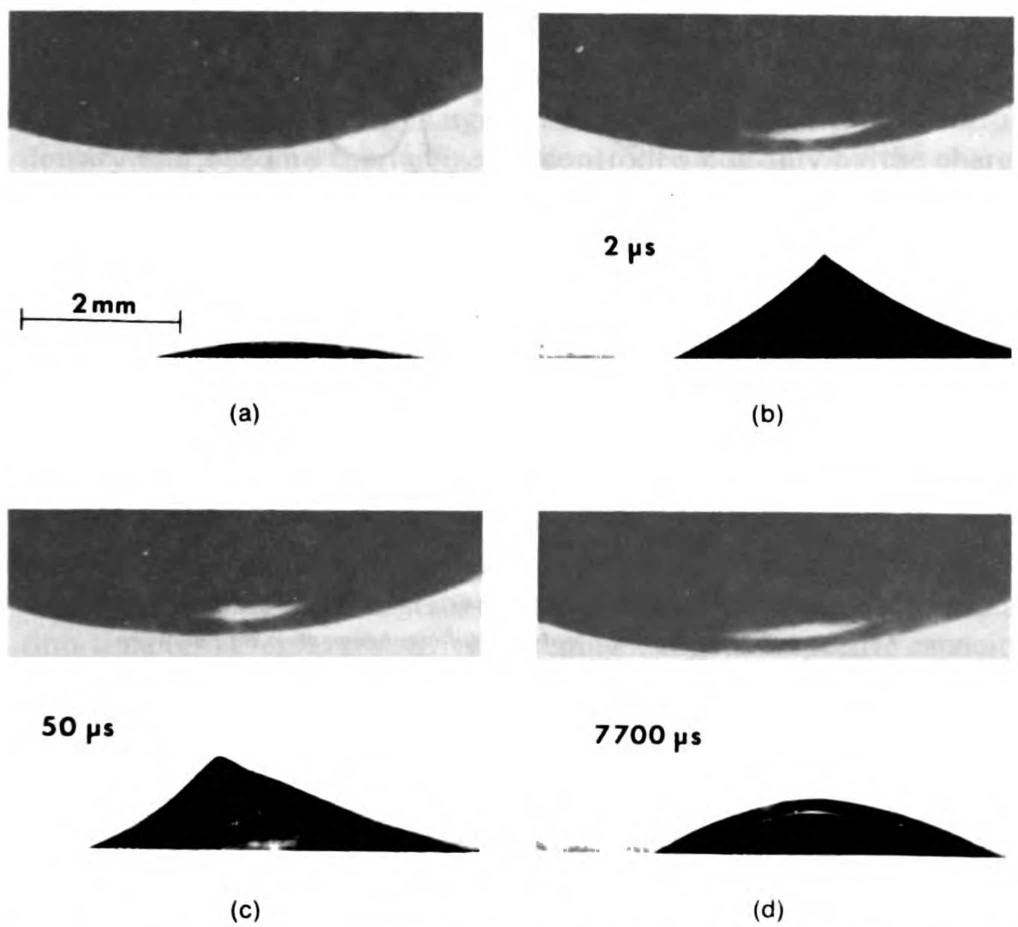

Figure 8 – Stressed water surface at several times. (a) Shows the spheroidal equilibrium shape that protrudes over the flat water surface at a maximum voltage just under 8 kV. A small voltage increase changes from shape (a) to (b) within a few milliseconds. A spark takes place 2 μsec before picture (c). Tap water of 2000Ω-cm resistivity was used (d).

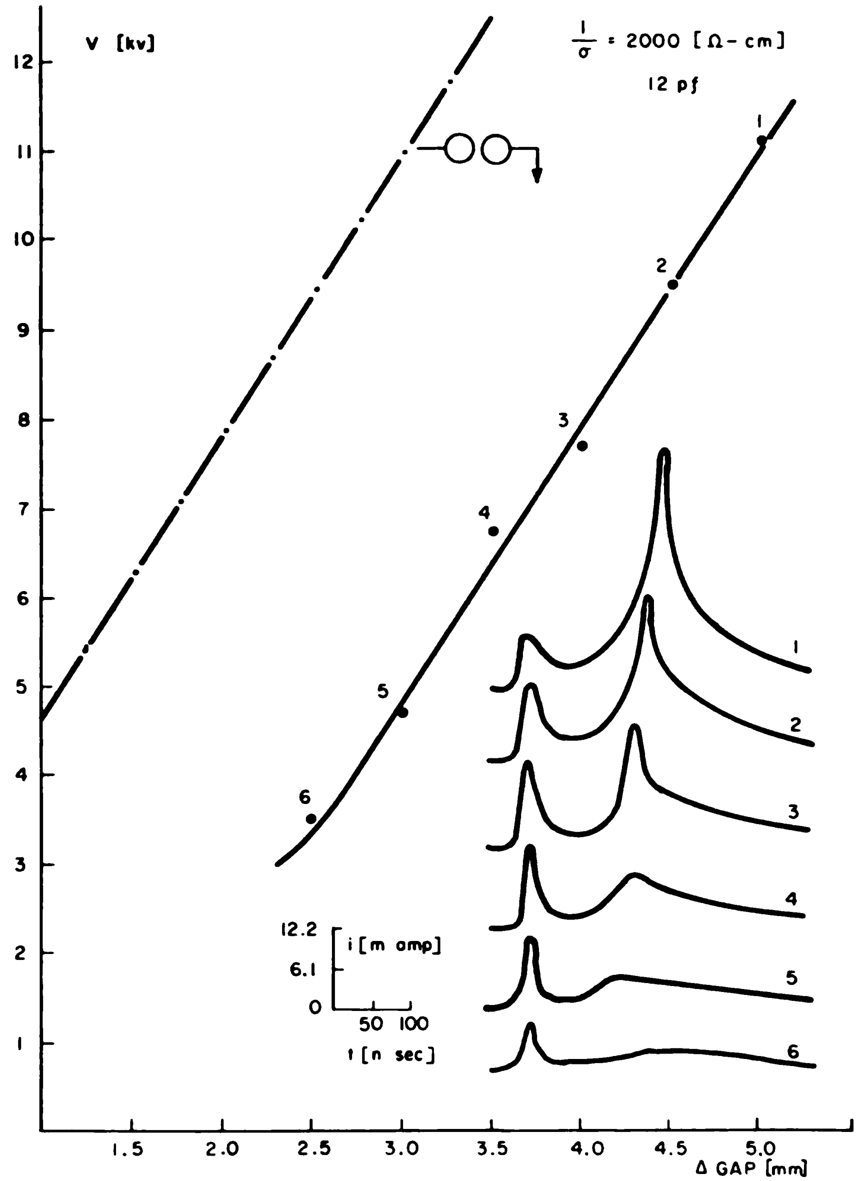

Figure 9 — Comparison of the voltage required to produce an electrical discharge using either two metal spheres 2 cm in diameter (Reference 16), or a water-to-meta-sphere electrode configuration. The gap separation, for the water-metal arrangement, is that between the flat water surface and the top metal sphere with no applied voltage. The oscilloscope current traces obtained with different gap separations are reproduced and identified by corresponding numbers in the graph for the water-metal case.

are, however, different than those obtained using point-to-plane small metal gaps where the first streamer leads to a spark and the whole event is over in times smaller than 40 nsec (such traces look like that in Figure 3 except that there is a hump on the rise time). The current traces in Figure 9 show, instead, an initial streamer followed by a sharp current decrease that leads to a second current pulse in about 150 nsec. The initial streamers are all roughly of the same amplitude, as expected by considering that the field that changes a spheroid into a cone depends on the surface properties of the water (surface tension, polarization) and not on the applied voltage or gap separation. That is to say, the same local field intensification is always produced by the change in shape of the water; hence, the same initial streamer discharge results in all cases. The amplitude of the second current pulse varies roughly as the square of the gap separation, therefore, as the square of the applied voltage, because these two are linearly related as shown in the graph (Figure 9). The second pulse is then proportional to the stored energy and is the one that actually discharges the capacitor.

It is evident that the charge liberated by the initial streamer interacts with the water surface and affects the ionization process. Furthermore, the existence of two separate current pulses indicates that the electric field in the gap is reduced by surface charge deposited by the initial streamer on the water. As this charge leaves by conduction through the liquid, the field again increases, and ionization is enhanced, allowing the capacitor to be discharged. It follows that the ability of the discharge channel to produce critical electron density and become thermalized is controlled not only by the charge on the capacitor but also by the conductivity of the water being used.

The conductivity of the water determines the period of time when the charge deposited on the surface affects the electric fields in the gap. Consequently, the separation between current peaks is dependent on changes in conductivity. In Figure 10 we show a plot of the time between peaks versus the resistivity (the inverse of conductivity, $1/\sigma$) of the water used. The stored energy is larger than the minimum with metal electrodes (0.47 vs 0.38 mJ), but no ignitions are produced. Corresponding current traces for the points in the graph are displayed in Figure 10 together with a plot of the computed relaxation time (ϵ/σ) versus resistivity assuming a constant specific capacity [$\epsilon = (80)\ 8.85 \times 10^{-12}$ F/m]. At low resistivity the current pulses exhibit a metal-like single-pulse behavior (traces 1 and 2 in Figure 10). Then as the resistivity increases, two current pulses appear (like those in Figure 9) with continued current and light emission between them (traces 3-10 in Figure 10). Finally, as the time between the pulses increases with resistivity, the current between them becomes negligible and the photomultiplier shows a corresponding dark period, thus evidencing that the surface charge on the water stays long enough and is strong enough to stop the ionization in the gap. Note that this happens only when the time between current pulses

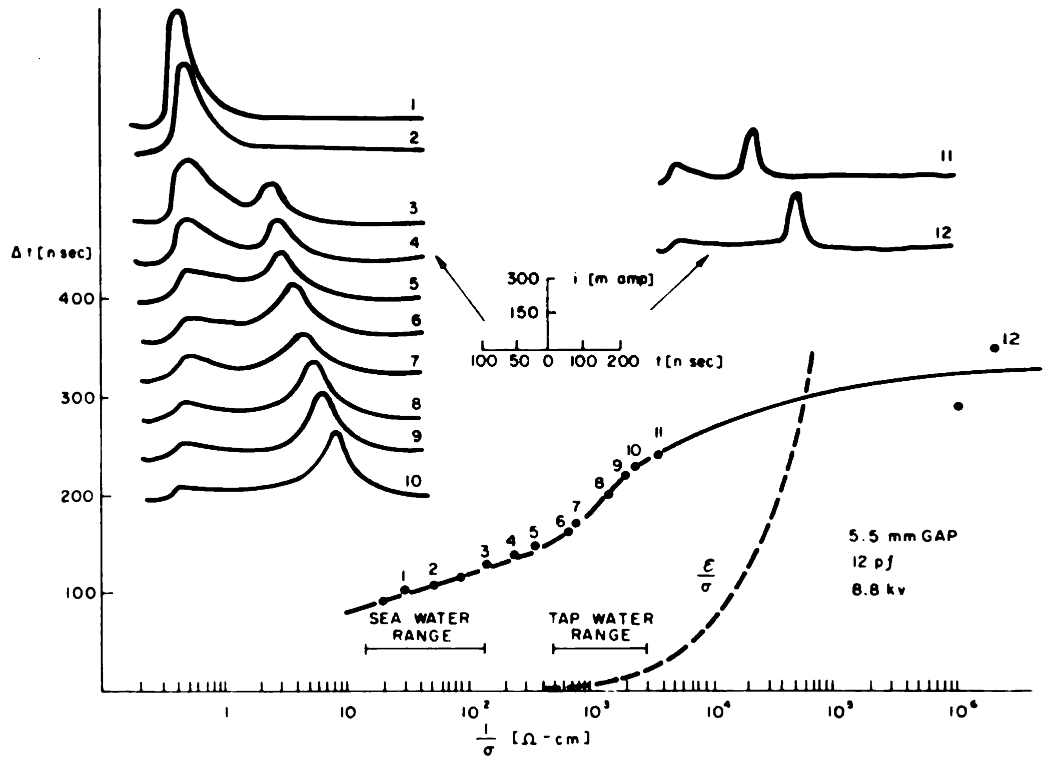

Figure 10 — Time between current pulses as a function of resistivity compared to the computed relaxation time. The gap separation is 5.5 mm between the metal surfaces shown in Figure 1. The thickness of the water film varies between 1.4 and 1.6 mm in all our tests. The range of resistivity of sea water as reported by Dorsey (Reference 17) and that measured in our tap water for all tests are also shown for reference purposes. All discharges are not thermalized.

becomes comparable with the relaxation time of the water (to the right of point 11 in Figure 10). Depending on the resistivity of the water we can then distinguish two different regions with different behaviors: at high resistivity the initial streamer completely stops the discharge; while at low resistivity the ionization never stops and the rate at which it takes place is affected by the initial streamer. This includes the low-resistivity single metal-like pulses (1 and 2 of Figure 10), as we will now show.

A single-pulse behavior indicates that the charge produced by the initial streamer can be removed fast enough through the liquid in such a way that the surface charge on the water does not reduce the ionization process in the gap. However, there exists a characteristic RC time for the circuit that determines the rate at which energy can be fed into the air gap. Let us consider the tip of the water cone as a cylindrical volume with a length and radius of the order of Taylor's filaments (10 μm). Then, the effective resistance of the water used for trace 1 in Figure 10 is computed as $1.02 \times 10^4 \Omega$. This resistance, together with the capacitance used (12 pF), represents a relaxation time for the electrical circuit of 122 nsec. Therefore, in this time only 1/e of the total available charge goes into the discharge gap. The number is 3.8×10^{-8} C and compares favorably with the area measured under trace 1. which is 3.6×10^{-8} C. Note also that 122 nsec is of the right length to account for the duration of the current trace. However, the total charge transferred represents only a density of 1.5×10^{16} electrons cm^{-3}. That is about six times lower than the value required for thermalization in the channel. Due to the small capacity used, the charge transferred is, nevertheless, a significant amount for the reduction of voltage across the gap ($dQ/C=3200$ V). Therefore, the field is gradually reduced, and ionization stops before the channel is able to heat up. Note that most of the energy stays in the capacitor and is not transferred to the gas to produce an ignition even though its value is larger than the minimum value using metal electrodes.

Increasing the capacitance of the system increases the charge transferred in the initial stages of the accumulation process in the gap. [$Q = Q_o \exp(-t/RC)$]. Consequently, the ionization process is not stopped before thermalization occurs. The effect is demonstrated in Figure 11, which shows the traces obtained with a fixed but larger capacity (9.2 times that in Figure 10). Again the traces are for different resistivities, but we plot the peak current and the charge (area) under the first current oscillation. Traces 1-4 correspond to the low-resistivity single-pulse behavior seen in traces 1 and 2 of Figure 10. Pulses 5-8 correspond only to the second current pulses. This is because the first small streamer pulse produced in the high-resistivity regime (such as No. 12 in Figure 10) is eliminated by adjusting the oscilloscope in order to be able to see the shape of the decay curve for the second pulse. In Figure 11 all traces are thermalized discharges. The behavior of the first four pulses is interesting because it shows a constant charge transfer of 1.8×10^{-7} C during the single pulse of the discharge. This charge is 5.4 times smaller than the available charge on the capacitor, but it is of the magnitude required for thermalization. It corresponds to 2.4×10^{17} electrons cm^{-3} in a 0.13-cm-long discharge channel that is measured from the tip of the water cone to the metal sphere. The time interval involved is also about twice the value measured when metal surfaces are used (compare to Figure 3). It is clear that to thermalize the single-pulse characteristic of high conductivity (e.g., 1 and 2 in Figure 10), it is necessary to increase the capacity in order to increase the amount of charge transferred per unit time to a value consistent with the RC of the circuit and the procurement of a critical electron density. Note that although the current rapidly decreases with a resistivity increase, the time variation of the current compensates for the change in such a way as

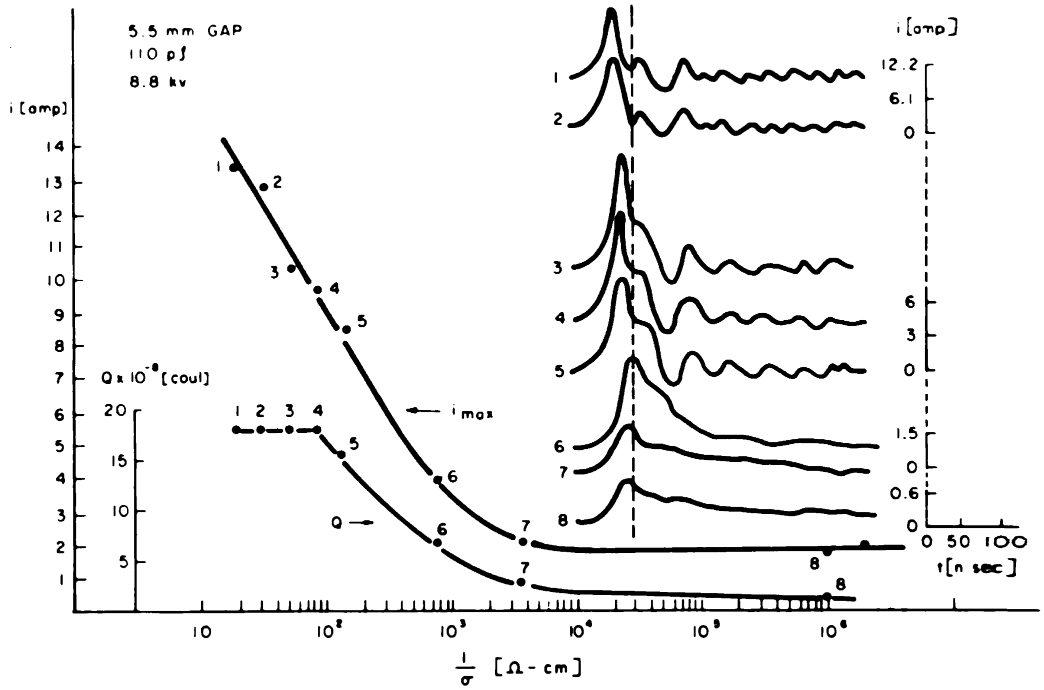

Figure 11 – Peak current of largest pulse and charge transferred as a function of resistivity. The metal gap is 5.5 mm. The vertical line on the current traces is drawn at 85 nsec. Note that the conductivity and current ranges are different from those in Figure 10. All discharges are thermalized. In pulses 6-8 an initial streamer is eliminated by adjusting the oscilloscope triggering level.

to keep the total charge transferred constant (single pulses 1-4). This is, of course, in agreement with the critical electron density requirement.

Let us consider now the high-resistivity regime, where the electrical discharge actually stops between current pulses. As shown in Figure 12 the initial streamers are all the same, independent of the capacity used. This confirms that, as with solids, the first streamer can always produce enough charge to cancel the applied electric field and stop the discharge. Note that the separation between pulses is practically constant and that the effect of increased capacity is associated only with the amplitude and oscillations of the second current pulse. Visually the oscillations can be associated with bright surface discharges just as with the polyester film.

Conclusions

The concept of a minimum stored energy value that determines the ability of electrical discharges to produce ignitions, is suitable only under the restrictions of uniform electric fields and metal electrodes. Discharges produced with non-metal electrodes or with different geometrical configurations may be harmless even with stored

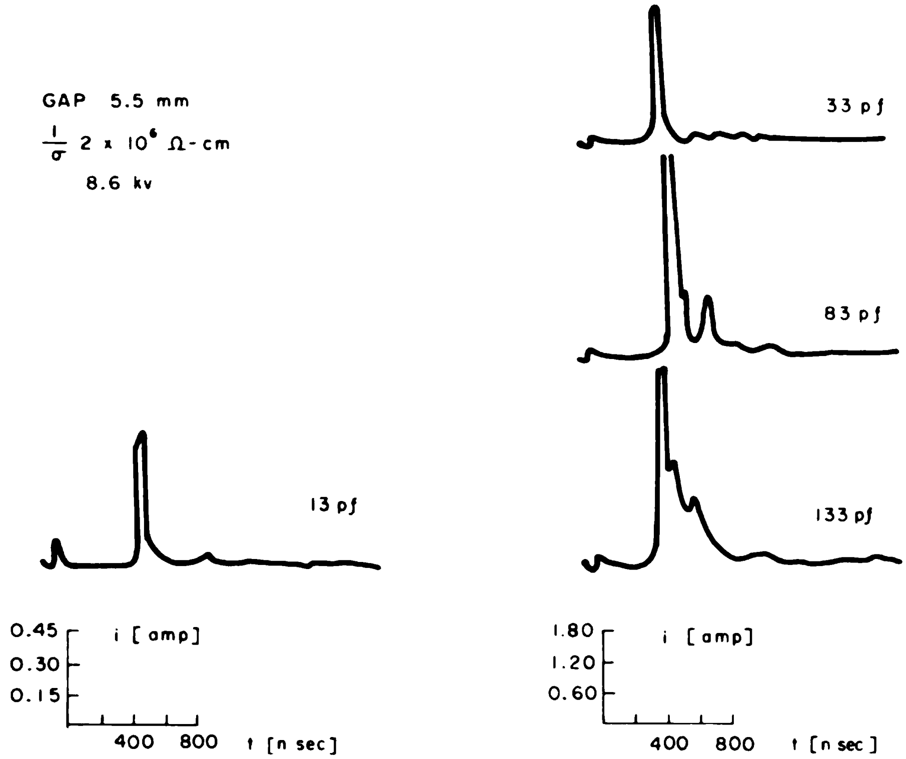

Figure 12 — Current traces of discharges in a water-metal gap using low-conductivity water and different capacitors. The distance is 5.5 mm between metal surfaces as shown in Figure 1. The discharges at 83 and 133 pF produce ignitions.

energies that are very large compared to the minimum value. For instance, corona discharges are always harmless regardless of the energy supply. Ignitions are determined exclusively by the ability of an electrical discharge to heat the gas. This happens when the applied electric field transfers heat energy into the channel left by an initially produced streamer and is possible only when a critical electron density is reached. As expected, this critical value corresponds to the number at which the electrons in the discharge hold a total kinetic energy comparable to the thermal energy of the neutral gas molecules. The number is about 10^{17} cm^{-3} for the gas mixture used, and is independent of geometry or electrode material. It constitutes a more physically meaningful criterion to determine ignition ability than an absolute energy value and corresponds to the number at which breakdown theory predicts and measures the properties of a weak plasma state. The interaction of the initially produced streamer with the electrodes and the geometry determines the ability of the applied field and the stored energy to produce the critical electron density, hence the ignition. With metals the charge produced in the head of the streamer is instantaneously absorbed by the surface; consequently, the transfer of energy to the gas is optimized and the work done in the procurement of a critical electron density corresponds precisely to the minimum energy value. With solids the charge from the initial streamer stays in the surface long enough to stop the discharge in the gap. No ignitions take place unless this charge is removed by subsequent surface discharges. However, with a polarity reversal this same accumulation of charge may lead to thermalization at an applied voltage that is much smaller than the value required with metal electrodes. The effect depends on the conductivity of the solid and remains active even after days with the better dielectrics.

Liquids deform under electric stress and this modifies the ignition properties. Liquids of low surface tension form thin filaments that produce either harmless coronas or no discharges at all but merely a high-resistance connection between the electrodes used. Liquids of high surface tension produce discharges as a result of a geometrical change that occurs at a field lower than the value for ionization of the air. The ignitions are therefore always associated with higher capacities than in a uniform field (larger objects, thinner dielectrics). Depending on the conductivity of the liquid, the discharge is thermalized either by gradual accumulation of the critical electron density with continued ionization or by a new discharge with a period of no ionization in between.

In all cases the type of discharge produced and its ability to ignite can be determined by analysis of oscilloscopic recordings of the current as a function of time. Also, the discharge current traces show that except for metals and uniform fields ignitions always involve the propagation of discharges in nonuniform electric fields. This means that previous studies of ignition by electrical discharges have almost always consistently excluded the discharges that are most interesting in terms of practical hazards.

In long sparks where steps are produced, the initial streamer will be eventually affected by the space charge left behind it and will die unless its channel becomes thermalized. However, when the channel becomes thermalized, any original geometry will change to a highly asymmetric one, and a strong pulsed voltage will be produced at the propagating tip. Consequently, the subsequent streamer stage propagates like a pulsed strongly branched streamer discharge at the end of each step. It seems, then, that branching and stepping are both associated with thermalization, and that if thermalization does not occur, long sparks, the same as small sparks, will not be produced.

References

1. Lewis, B., and von Elbe, G., *Combustion, Flames, and Explosions of Gases*, 2nd ed. (Academic, New York, 1961).

2. Barreto, E., State University of New York ASRC Publication No. 172, 1972.
3. van der Meer, D., 2nd International Conference on Static Electricity, Frankfurt, 1973 (unpublished). Also, American Petroleum Institute, Rpt. No. 74-2247, Final Report Tanker Accident Study Committee (Nov. 27, 1974).
4. Whittman, R.E., Lightning and Static Electricity Conference, Las Vegas, Nevada, 1972 (unpublished).
5. Brick, R.O., Lightning and Static Electricity Conference, Las Vegas, Nevada, 1972 (unpublished).
6. Potter, A.E., and Baker, B.R., Lightning and Static Electricity Conference, Las Vegas, Nevada, 1972 (unpublished).
7. Reynolds, S.I., General Electric Report No. 67-C-059, 1967 (unpublished).
8. Loeb, L.B., Electricity Coronas (University of California Press, Berkeley, 1965).
9. Reynolds, S.I., Nature (Lond.) 183,671 (1959); AIEE Commun. Electron. (1960).
10. Bertein, H., 2nd International Conference on Static Electricity, Frankfurt, 1973 (unpublished).
11. Murooka, Y., and Kovama, S., *J. Appl. Phys.* **44**, 1576 (1973).
12. Creswell, R.A., and Perlman, M., *J. Appl. Phys.* **41**, 2365 (1970).
13. Taylor, G.I., *Proc. R. Soc.* **A 313**, 453 (1969).
14. Barreto, E., *Aerosol Sci.* 2, 219 (1971).
15. Azad, A.K., and Latham, J., *J. Atmos. Sci.* **25**, 66 (1968).
16. Meek, J.M., and Craggs, J.D., *Electrical Breakdown of Gases* (Oxford U.P. Oxford, England, 1953), p. 313.
17. Dorsey, N.E., *Properties of Ordinary Water Substance in All Its Phases* (Reinhold, New York, 1960).

(Continued from Page 9)

In preliminary lab tests, the friction behavior of Nylon-11 at contact pressures up to 120,000 pounds per square inch (8 kilobars) at room temperature was measured. The friction coefficient was unusually small or only about one-half of that of fluoroethylene films measured in the same test apparatus under comparable conditions.

Nylon is a generic term scientists use for polymides which are long-chain synthetic polymeric amides that have recurring amide groups as an integral part of the main polymer chain. Nylon-11 is distinguished from other commercially available nylons by a relatively low melting point (186 C), broad processing temperature range, low specific gravity (1.04), low moisture absorptivity (1.9%), and high flexibility. It is highly solvent resistant and has found extensive application as a corrosion resistant coating.

Because of the solvent resistant characteristics of Nylon-11 films, they are easily prepared by using a dry powder coating technique.

Research Notes

Fiber Optics used for Real-Time Dosimeters

Naval Research Laboratory (NRL) scientists have advanced the technology of dosimetry (radiation detection) through the use of optical glass fibers to develop new, improved and inexpensive dosimeter systems. In studies sponsored by the Office of Naval Research the glass fiber detection systems were found to be at least 100 times more sensitive to gamma rays than conventional bulk glass dosimeters currently in use. The successful laboratory research on glass fiber dosimeters may lead to the development of detection systems that will provide real-time measurements of radiation aboard ships and aircraft that either contain radioactive sources or are subject to external radiation from gamma rays. Such dosimetry systems could be valuable to the civilian community, providing a low cost, real-time detection system in work areas where nuclear power sources are used to produce energy.

NRL has long been interested in fiber optics technology, which is essentially the transmission of information or images with light through bundles of glass of approximately 100 microns diameter by total internal reflection. To date, communication applications have dominated work in the fiber optics field. However, a team of solid-state scientists at NRL recently decided to use the glass fibers to develop experimental dosimeters.

Glass darkens upon exposure to high-energy radiation such as gamma rays. When exposed to the same amounts of radiation, some glasses darken more than others, and thus would serve as better dosimeter materials. By drawing such glasses into long fibers, the path which light can travel through the glasses is greatly increased; consequently, very small amounts of darkening (radiation) are detectable. The fibers may be coiled so that a long light path can be compressed into a minimum amount of space.

If a number of such wave guides or fibers are bundled together, the configuration may be used as a compact, low-cost, highly sensitive dosimeter to provide continuous real-time measurements of radiation exposure.

In the NRL system, bundles of coiled fibers are used in conjunction with available solid-state light sources (light-emitting diodes) and photodiode detectors to monitor radiation in real-time for ships or aircraft.

The amount of light received at the system terminus would be monitored by photodiode detectors whose output could be recorded graphically, thus providing a permanent visual record of any fluctuations. Because irradiation of the fibers reduces their ability to transmit light, the exposure of the system to radiation would cause a measurable reduction in the photodiode output, which would appear on the graph.

Currently, in NRL's ongoing research into the application of low-loss fiber optics for dosimeter systems, the response of a variety of fiber materials to radiation is being evaluated. These studies will hopefully lead to dosimeters of even greater sensitivity.

Sub-sea Permafrost

At a time when extensive offshore development is anticipated in Alaska, the occurrence and characteristics of sub-sea permafrost along Alaska's coastline becomes increasingly important. In April Dr. Robert Lewellen began his fifteenth year doing basic research into permafrost at the Naval Arctic Research Laboratory. Dr. Lewellen will concentrate this year on the nature of sub-sea permafrost in the Tapkaluk Islands fifteen miles east of NARL. His research is sponsored in part by the Office of Naval Research.

The Naval Arctic Research Laboratory will assist Dr. Lewellen in establishing a research site on the ice. This site will consist of three sled-mounted buildings: a living hut, a laboratory and a building to house the diamond core drill used to obtain sub-sea cores. With him at the research site will be Mr. Simeon Akpik and Mr. Joe Ningeok, both NARL employees and arctic veterans experienced in using heavy equipment. Drilling for sub-sea cores takes place while the shorefast ice is safe and thick–from the middle of March until the end of May.

After analyzing numerous cores obtained on or along the shore as well as offshore, Dr. Lewellen has found permafrost throughout the cores down to a maximum of 300 feet below the surface, which was the extent of his drilling depth. Throughout his years of gathering baseline permafrost data in the arctic he has devised drilling techniques which are environmentally safe. This knowledge will be pertinent to the establishment of engineering and design criteria for arctic offshore public works or industrial development and is made available to the public domain.

Dr. Lewellen, an independent contractor of arctic research, plans to continue studying permafrost along the presently eroding arctic coastline, in the shallow bays and lagoons and around the barrier islands, as well as the deeper waters at sea from Cape Beaufort to Demarcation Point.

Meteorologist Modifies Air Structure Measuring Device

To most people, the atmosphere is either blue sky or clouds, or a combination of both. Not so for Louisiana State University (LSU) associate professor Dr. S. A. Hsu! To him the atmosphere is a complex of layered air with ever-changing meanings.

A research meteorologist of the LSU Coastal Studies Institute, in the Center for Wetland Resources, Dr. Hsu's particular interest is the atmospheric structure of air-land-water interfaces–in other words, the air over coasts. He describes his specialty as "mesoscale processes" to distinguish it from the study of large, synoptic weather systems usually analyzed by weather forecasters.

Recently Dr. Hsu began experiments with equipment that may revolutionize the study of atmospheric structure. He's modifying an acoustic sounder (which measures atmospheric conditions by temperature variations) to produce a portable model.

The acoustic sounder sends a pulse of sound straight upward. As the pulse hits an atmospheric boundary between the layers of differing density and temperature, some of the energy is bounced back to earth as a sort of echo, while the rest passes on to the next interface, and another partial reflection. This process continues until all the energy in the upward-traveling pulse is spent. The echoes are recorded on a chart, from which scientists can determine the heights and thicknesses of atmospheric layers.

The major drawback to such systems is their immobility, Dr. Hsu said. Present methods require the establishment of fixed measuring stations at various ground sites and a correlation of profiles between sites. A detailed picture of the layers is not produced, Dr. Hsu says, because the layers of the atmosphere may undulate between measuring stations. Some land areas warm faster than others—for example, where there are many buildings or a large concentration of population. As the warm air rises, the surrounding air sinks, producing corresponding changes in atmospheric layers. This phenomenon is particularly relevant along coastlines, where the temperature difference between land and sea creates unique atmospheric structures.

In Dr. Hsu's experiments the sounder's dish-shaped antenna, four feet in diameter, is maintained on top of a truck or boat, so that profiles along ground traverses can be mapped quickly and in fine detail. Although his primary purpose is to achieve—with other Coastal Studies Institute scientists—a comprehensive understanding of the interactions between land, air, and sea along a particular coast, Dr. Hsu says the movable system will work anywhere. The instrument will have its first application this Spring when a team of LSU researchers studies the northeastern coast of Brazil.

Dr. Hsu stresses that his field of expertise has particular relevance to man's coastal and nearshore marine development. For instance, many complicated factors enter into the selection of sites for such major developments as airports or nuclear power plants. Some important ones are related to the weather system—the wind regime, air turbulence, fog, smog, aerosols, and temperature. An overall analysis of these weather factors, evaluated with the aid of various formulas that Dr. Hsu has developed for predicting process interactions, can lead to the identification of the most suitable site.

New Technique Improves Air Filtration

Naval Research Laboratory scientists have taken an industrial-grade, fiberglass air filter, applied an electric voltage to it, and wound up with a filter ten times more effective than it was.

George H. Fielding, the principal investigator for this Environmental Protection Agency funded program, says "Unlike electrostatic precipitators, with which it is occasionally confused, the NRL 'dielectrophoretic' filter requires only very low current and power. Also the system requires no more voltage than the power supply of a small portable TV set."

The new technique uses high voltage to establish an electric field across the fiberglass filter. This increases the efficiency of the filter for a 0.3 micron (0.0003

U. S. GOVERNMENT PRINTING OFFICE : 1975 O - 588-356

millimeter) aerosol from a normal 68 percent to 98 percent. Cigarette smoke falls in the 0.3 to 0.7-micron range. For larger aerosols of one micron, the filtration efficiency increases from 78 to 99 percent.

In the NRL technique, the power supply is connected to the metal screens on either side of the fiberglass filter. The electric field thus set up between the screens polarizes the aerosols, while the glass fibers distort the electric field. This accelerates the particles toward the fibers, where they are retained.

The method has many potential applications, especially for shipboard use. Cigarette smoke, for example, an aerosol that has been particularly difficult to filter, is especially troublesome in submarines and other closed spaces. This makes the future of dielectrophoretic filters in such environments quite promising.

Other potential applications for the new technique include: prefiltration to protect the very costly filters in nuclear reactor spaces, cleanroom filters for hospitals or sensitive electronics areas, and inlet air filters for other nuclear, biological, and chemical protection.

NAVAL RESEARCH REVIEWS publishes highlights of research conducted by Navy laboratories and contractors and describes important naval experimental facilities. Manuscripts submitted for publication, correspondence concerning prospective articles, and changes of address, should be directed to Code 730, Office of Naval Research, Arlington, Va. 22217. Requests for subscriptions should be directed to the Superintendent of Documents, U.S. Government Printing Office, Washington, D.C., 20402. Subscription price: $6.50 per year in the U.S. and Canada; $8.15 per year, foreign; $0.55 per individual copy. The issuance of this periodical approved in accordance with Dept. of the Navy publications and printing regulations.

Editor: WILLIAM J. LESCURE

NAVSO P-510

Associate Editors:

A. R. LAUFER, ONR PASADENA

A. R. DAWE, ONR CHICAGO

A. L. POWELL, ONR BOSTON

D. A. PATTERSON, NAVAL RESEARCH LABORATORY

IN THIS ISSUE

VOL. XXVIII, NO. 7

Cover Caption

An electrical discharge mode in the laboratory over a charged mylar surface. See page 10.

DEPARTMENT OF THE NAVY
OFFICE OF NAVAL RESEARCH
ARLINGTON, VA. 22217

OFFICIAL BUSINESS

PENALTY FOR PRIVATE USE, $300.

POSTAGE AND FEES PAID
DEPARTMENT OF THE NAVY
DoD-316

U.S.MAIL